



## COLLAPSE ANALYSIS OF URM CAVITY-WALL BUILDINGS WITH DIFFERENT GROUND FLOOR OPENING LAYOUTS

D. Malomo<sup>(1)</sup>, R. Pinho<sup>(2)</sup>, C. Morandini<sup>(3)</sup>, A. Penna<sup>(4)</sup>

<sup>(1)</sup> Consultant, Mosayk Ltd (Pavia, Italy), [daniele.malomo@mosayk.it](mailto:daniele.malomo@mosayk.it)

<sup>(2)</sup> Technical Director, Mosayk Ltd; Full Professor, University of Pavia (Pavia, Italy), [ruipinho@mosayk.it](mailto:ruipinho@mosayk.it)

<sup>(3)</sup> Doctoral Student, University of Pavia (Pavia, Italy), [chiara.morandini02@universitadipavia.it](mailto:chiara.morandini02@universitadipavia.it)

<sup>(4)</sup> Associate Professor, University of Pavia (Pavia, Italy), [andrea.penna@unipv.it](mailto:andrea.penna@unipv.it)

### **Abstract**

The terraced house building typology, which typically consists of low-rise unreinforced masonry (URM) constructions with cavity walls, rigid floor diaphragms and timber roof, is largely widespread in the Groningen region (The Netherlands), now exposed to low-intensity ground motions due to gas extraction. Recent experimental evidence has shown that, in addition to the lack of seismic details, the presence of large openings at the ground floor makes these structures particularly vulnerable towards horizontal actions. In this paper, detailed micro-models, developed within the framework of the Applied Element Method, are employed to extend experimental findings through a comprehensive study on the impact of ground floor openings percentage on the dynamic response of cavity-wall systems representative of the typical Dutch terraced houses, up to complete collapse. After a preliminary calibration with full-scale shake-table test results, the behavior of two additional models, which can be regarded as representative of lower and upper bounds with respect to the extent of ground floor openings of the shake-table-tested prototype, is investigated considering the same experimental loading protocol. Preliminary results confirm that the percentage of ground floor openings may affect significantly the dynamic performance of typical Dutch terraced houses, with the overall strength capacity of the latter decreasing with increasing openings percentage, which also causes deformations and failure mechanisms to concentrate on the ground floor.

*Keywords: Unreinforced masonry, cavity-wall systems, openings, shake-table, Applied Element Method*



## 1. Introduction

Unreinforced masonry (URM) terraced houses represent a large portion of the building stock of the Groningen region (The Netherlands), recently exposed to induced-seismicity phenomena. They typically come in the form of low-rise residential buildings characterized by the presence of reinforced concrete (RC) floor diaphragms, timber roof and cavity-walls, constituted by the assembly of a loadbearing (calcium silicate - CS - brick) inner leaf plus an outer (clay - CL - brick) veneer with only aesthetic and insulation functions. Their design, originally not conceived for earthquake-resistance, often features the presence of large openings at the ground floor. This aspect, combined with the lack of any specific seismic consideration or detailing, further increases the associated vulnerability towards horizontal loading.

For the above reasons, the investigation of the seismic behavior of terraced house buildings has lately become the focus of a comprehensive experimental campaign [1] aimed at providing a foundation on which to base risk assessment strategies and the development of potential retrofitting solutions. Of particular interest are the shake-table tests of two full-scale cavity-wall two-story building prototypes representative of the end-unit of a set of typical Dutch terraced houses; EUC-BUILD1 [2] and EUC-BUILD6 [3]. The main distinction between such test specimens was in the size of their ground-floor openings (purposely wider in the case of EUC-BUILD6), which resulted in markedly different experimentally-observed responses in terms of both hysteretic curves, failure mechanisms and damage patterns.

In this work, taking as a reference the previously-validated strategy presented in [4], where adequate agreement among experimental outcomes and numerical counterparts of shake-table-tested cavity-wall building specimens (including EUC-BUILD1) was found, a refined Applied Element Method (AEM)-based model of EUC-BUILD6 is developed and preliminarily calibrated through comparison against available experimental outcomes. To extend laboratory findings, given the encouraging results obtained, analogous assumptions were also considered for the development of a number of models subjected to the same experimental loading scheme in which, parametrically, the area of ground floor openings was varied.

## 2. Applied Element modeling of URM Dutch terraced houses

The standard formulation of AEM, developed by [5,6,7] for simulating controlled demolition processes, can be easily adapted for simulating the mechanical response of URM elements and large-scale constructions, as shown by recent applications (e.g. [8, 9, 10]). According to the AEM, each unit is modeled as a rigid body, carrying only mass and damping of the system, which interacts with the adjacent ones by means of equivalent interface zero-thickness springs, representing unit-mortar mechanical properties according to a simplified micro-modeling approach [11], as depicted in Fig. 1(a).

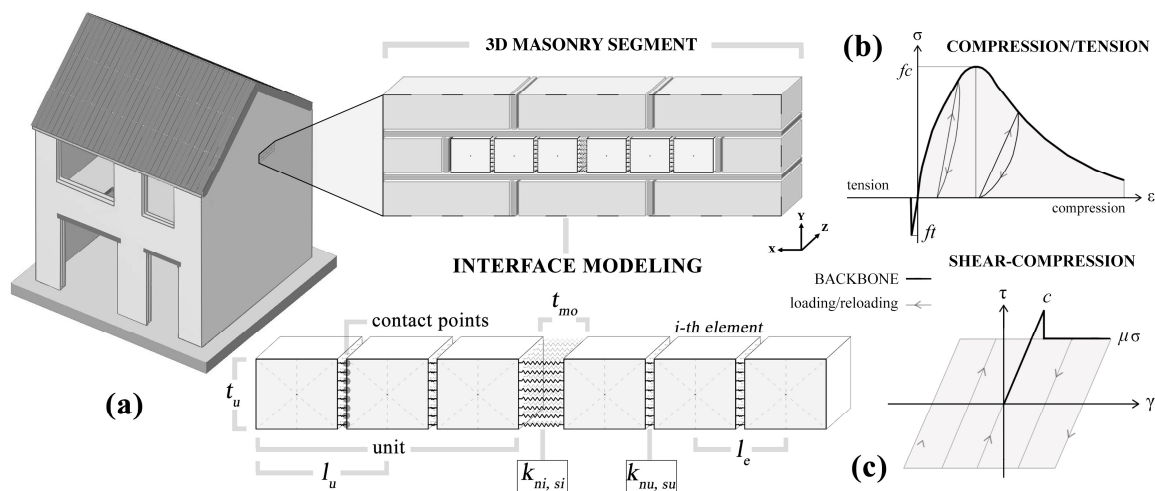


Fig. 1 (a) AEM discretisation of a 3D masonry segment, (b) compression/tension and (c) shear sliding joint models



A post-peak cut-off criterion is commonly employed for spring tensile failure, whilst a nonlinear relation is assigned to normal springs for simulating progressive deterioration of compressive strength (see Fig. 1(b)). Shear damage is idealized through a Mohr-Coulomb-like bilinear law, neglecting any cohesion softening branch, which is set to zero right after reaching the maximum shear strength. Hence, the global nonlinear behavior of the assembly and the associated crack pattern evolution are obtained by considering the local failure of each spring according to the abovementioned criteria. Then, when a given amount of springs has failed and their stiffness is set to zero, contact between units is lost. The analytical description of both unit-to-unit ( $k_{nu}$ ,  $k_{su}$ ) and interface ( $k_{ni}$ ,  $k_{si}$ ) normal and shear spring stiffnesses, is reported in Eqs. (1)-(4), where  $d$  is the distance between two consecutive springs along the y-direction and  $j$  is spring spacing along z-direction, while  $E_u$ ,  $E_{mo}$ ,  $G_u$ ,  $G_{mo}$  stand for the Young's and shear moduli of unit and mortar respectively.

$$k_{ni} = \sum_{i=1}^j \left( \frac{l_u - t_{mo}}{E_u d \left(\frac{t_u}{j}\right)} + \frac{t_{mo}}{E_{mo} d \left(\frac{t_u}{j}\right)} \right)^{-1} \quad (1) \quad k_{si} = \sum_{i=1}^j \left( \frac{l_u - t_{mo}}{G_u d \left(\frac{t_u}{j}\right)} + \frac{t_{mo}}{G_{mo} d \left(\frac{t_u}{j}\right)} \right)^{-1} \quad (2)$$

$$k_{nu} = \sum_{i=1}^j \left( \frac{E_u d \left(\frac{t_u}{j}\right)}{l_e} \right) \quad (3) \quad k_{su} = \sum_{i=1}^j \left( \frac{G_u d \left(\frac{t_u}{j}\right)}{l_e} \right) \quad (4)$$

The AEM formulation also readily allows the assignment of equivalent mechanical properties to interface springs to describe the actual behavior of a wide range of connection types (e.g. nailed, friction, etc.) present in the EUC-BUILD6 building specimen, whose test results were used in this work as a reference for calibrating the AEM models considered in the parametric study. In what follows, the AE idealization of the main structural details of EUC-BUILD6 specimen, as well as relevant assumptions, are briefly summarized. Interested readers may refer to [4] for further details.

- Undertaking the approach proposed in [8], a number of empirical (i.e. [12, 13]) and theoretical [14,15,16,17] expressions were used to obtain first estimates of  $E_u$ ,  $E_{mo}$ ,  $G_u$ ,  $G_{mo}$ , where direct experimental values were not available. Then, the ensuing average is considered for modeling purposes and the associated shear moduli are obtained assuming material isotropy. These values will be given in the next sections, together with the experimental ones
- The gaps between the underneath of both 1<sup>st</sup> and 2<sup>nd</sup> floor RC slabs and the top edge of the non-bearing CS longitudinal façades are filled with mortar only after construction completion. Thus, their frictional resistance is likely to be limited due to lack of vertical compression, whilst the compressive strength was also likely affected by shrinkage phenomena; these two aspects have been accounted numerically by assigning reduced flexural and shear stiffness values to the corresponding interface springs
- To avoid the explicitly modeling of pull-in and pull-out phenomena of tie-elements connecting CS and CL leaves (which would have implied a very high computational burden), and since they typically failed within the CL mortar bonds, a bilinear constitutive law with post-peak softening branch and tension cut-off (experimentally-determined through quasi-static pull-out tests by Messali et al. [18]) was assigned to the CL wall-tie interfaces. On the CS panel side, instead, a linear elastic connection, characterized by the same flexural stiffness of the CS mortar, was employed
- A simplified modeling strategy was undertaken for simulating the response of the flexible timber roofs, which has been idealized as a continuous elastic membrane. Both shear and flexural in-plane stiffnesses have been selected taking as a reference the experimentally-inferred values reported in [19].



### 3. Model validation against full-scale shake-table test results

The EUC-BUILD6 building prototype (see Fig. 2) was tested at the shake-table of Eucentre and, as discussed in [3], consisted of a two-story URM structure with asymmetrically-distributed large openings (especially at the ground floor), RC diaphragms, timber roof and cavity-walls. It was 5.94 m large, 5.58 m wide and 7.83 m height, with a total mass of 47.2 tons. Considering the definition reported in the Groningen Exposure Database by Arup [20], according to which the opening percentage can be computed as the ratio between the width of the openings and the width of the façade, the longitudinal ground floor walls of EUC-BUILD6 are characterized by 80% (West) and 50% (East) opening percentages.



Fig. 2 (a) Ground floor plan (in cm), (b) EUC-BUILD6 and roof construction details [3]

The specimen was fixed to the shake-table and subjected to incremental uniaxial acceleration time-histories (with Peak Table Acceleration - PTA - ranging from 0.06g – EQ-20%, to 0.38g, i.e. EQ-133%, when the specimen reached near-collapse condition). A selection of the main masonry material properties (directly implemented in the model), including compressive strength of masonry  $f_{cm}$ , flexural bond strength  $f_w$ , cohesion  $c$  and friction coefficient  $\mu$ , obtained either through characterization tests on small-scale assemblies or using the abovementioned analytical expressions when experimental data were not available, is reported in Table 1:

Table 1. Experimental and inferred masonry material properties of EUC-BUILD6

	CS - density $\delta_m = 1837$ [kg/m <sup>3</sup> ]								CL - density $\delta_m = 1967$ [kg/m <sup>3</sup> ]							
	$f_{cm}$	$f_{cu}$	$f_w$	$E_m$	$c$	$\mu$	$E_u$	$E_{mo}$	$f_{cm}$	$f_{cu}$	$f_w$	$E_m$	$c$	$\mu$	$E_u$	$E_{mo}$
Avg [MPa]	10.1	19.8	0.28	6593	0.6	0.7	7029	6593	11.6	50.0	0.24	4436	0.3	0.6	9000	1126
C.o.V. [%]	0.06	0.18	0.32	0.09	-	-	0.4	-	0.29	0.10	0.52	0.29	-	-	0.2	-

As gathered from Fig. 3(a), the actual displacements at both floor and roof levels were captured adequately by the model, as well as the 2<sup>nd</sup>-floor soft-story global failure mechanism, although the 2<sup>nd</sup> floor deformation capacities along the positive direction have been slightly overestimated, particularly in the final test phases.

The general positive impression regarding the model performance is further confirmed from the hysteresis curves depicted also in Fig. 3(a), where the base shear capacities for each cycle appear in good agreement with their experimental counterparts. Similarly, actual and predicted final crack patterns (only cracks on CS loadbearing walls are displayed) are comparable, although the model slightly underpredicted the damage propagation in the spandrel elements and in the OOP-loaded transversal CS walls, particularly in the gables.

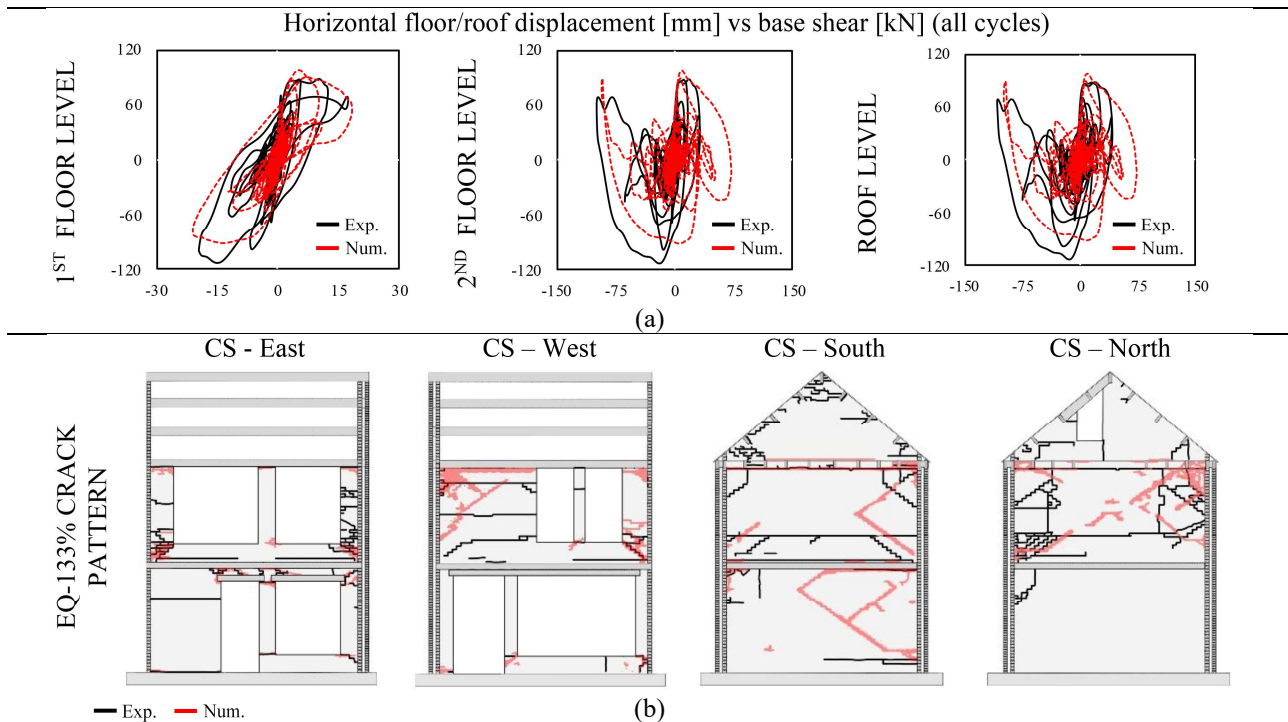


Fig. 3 (a) Exp. vs. num hysteretic response and building displacement profile, (b) final damage pattern of CS walls

#### 4. Influence of ground floor openings

In this section, a parametric study on the influence of ground floor openings percentage on the seismic response of a cavity-wall URM structure such as the tested house (i.e. EUC-BUILD6), is proposed. The same experimental loading protocol used for EUC-BUILD6 was employed, and the analyses were stopped right after the end of the final test phase (i.e. EQ-133%), which in the considered cases corresponded to the attainment of collapse conditions. In addition to the building specimen opening layout (hereinafter referred as EB6, characterized by 80% and 50% ground floor openings percentage in the West and East direction respectively), two different configurations (see Fig. 4), which can be regarded as representative of a lower and upper bound with respect to the extent of ground floor openings of EB6, are considered (it is noted that the ratio between the percentage of the openings of West and East façades was kept, in the range of the one of EUC-BUILD6, i.e. circa 1.6):

- Configuration C1 – in this case, rather than increasing the openings percentage of the initial structure, these were decreased to the following values: 50% for the West façade and 30% for the East façade
- Configuration C2 – then, keeping constant the ratio among openings percentage of West/East façade, the openings percentage was increased up to 90% and 60% for West and East façade respectively

In what follows, the results obtained for the three configurations described above are compared to each other, as well as to the experimental outcomes of the baseline structure (i.e. EB6), allowing one to readily gather the impact that modifying the façade layout varying percentage of openings has on the response of the building prototype.

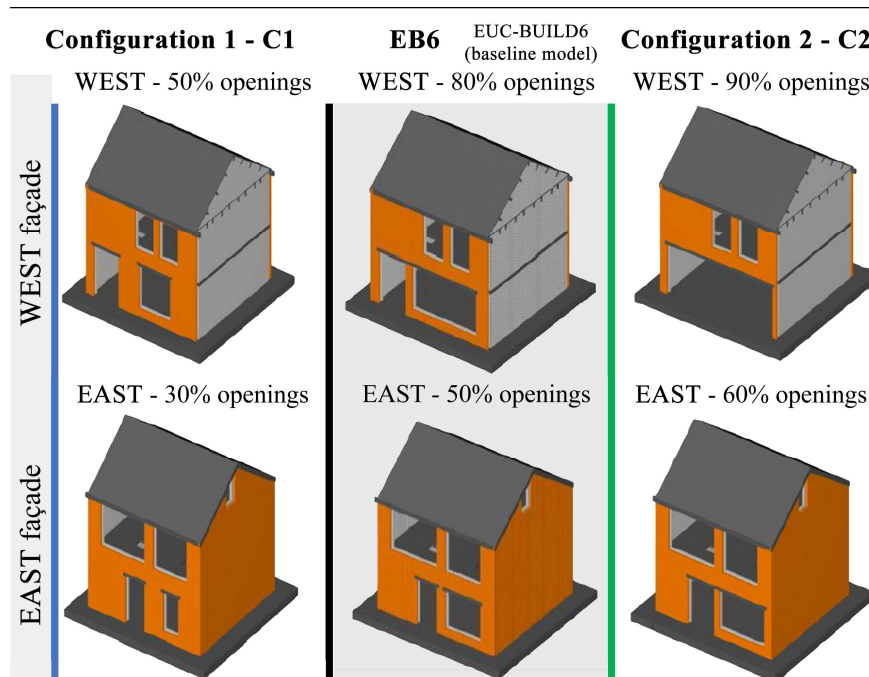


Fig. 4 Rendering of the models considered in the parametric study

As shown in Fig. 5(a), the lateral displacement capacity of the two models markedly decreases with increasing openings percentage. Indeed, in the case of C1, where the ground floor openings percentage has been reduced, the predicted first floor displacement along the negative direction of loading (i.e. South, where the CL transversal wall is not present) is almost 5 times smaller than the one of the baseline model and more than 10 and 15 times lower with respect to those predicted in the case of C2. The second floor and roof displacements for C1/C2, instead, appear comparable. This is because the models experienced different failure modes, as gathered from Fig. 5(b), and thus somehow “cancelling out” the expected dissimilarities.

From the hysteresis curves, it is also evident that the overall strength capacity of the specimens would tend to decrease with increasing openings percentage. Analogous considerations can also be made for what concerns the predicted crack patterns, which confirm the first and second floor soft-story types of response for C2 and C1, respectively. The latter only suffered limited cracks at the ground floor, particularly with respect to the out-of-plane damage in the CS transverse walls, which is close to negligible.

The reflections reported above are well epitomized by the plots in Fig. 6, where absolute maximum 1<sup>st</sup> and 2<sup>nd</sup> floor interstorey drifts (calculated as the relative displacement of the considered floor diaphragm divided by the story height underneath) for each cycle are plotted against the corresponding dimensionless base shear coefficient BSc (computed as the ratio between the absolute maximum recorded overall base shear and the weight of the specimen), and confirm that the extent of ground floor openings may affect significantly the dynamic performance of this specific type of URM cavity-wall buildings.

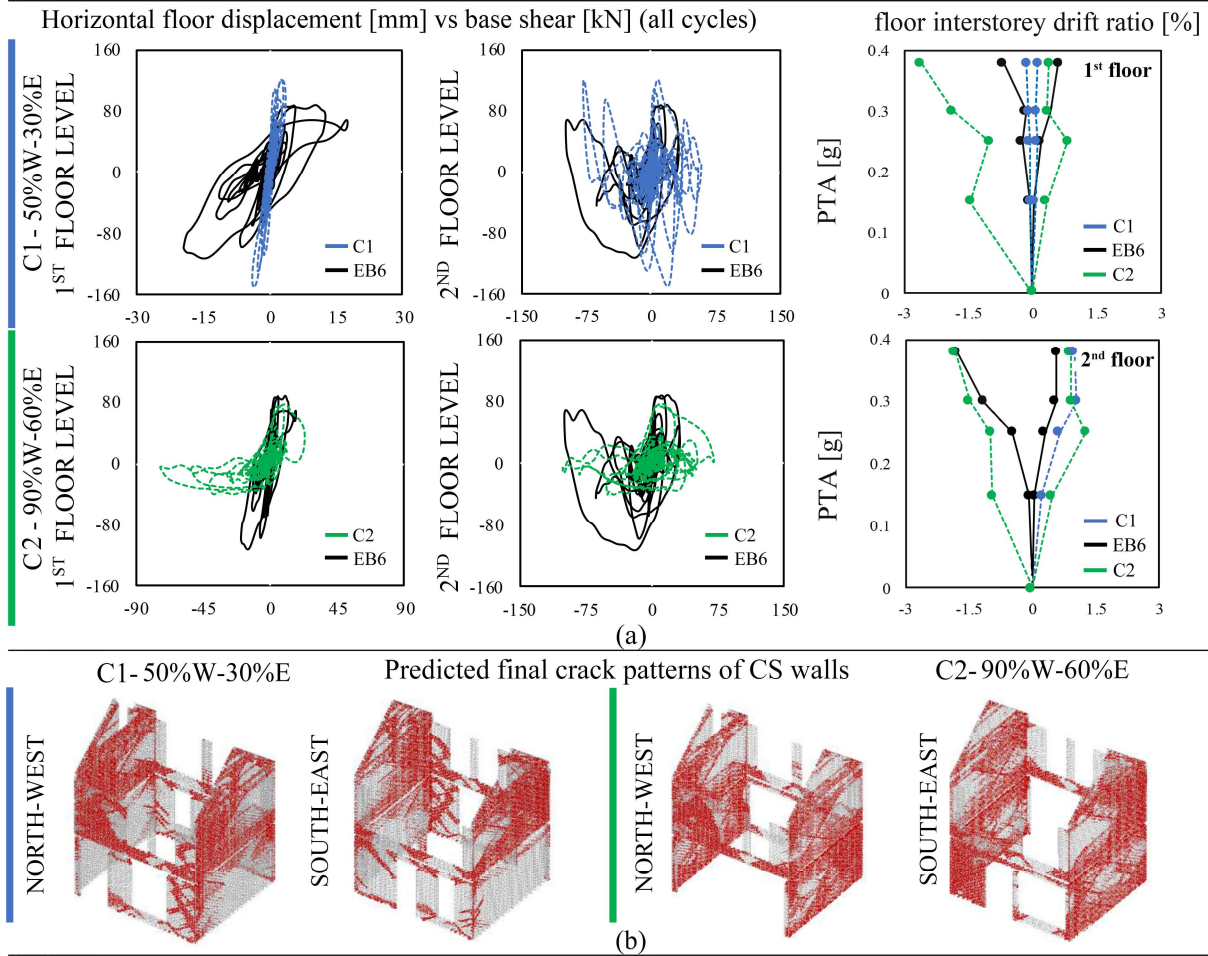


Fig. 5 (a) Predicted hysteretic response and interstorey drift ratios for configurations C1/C2 and comparison with those inferred experimentally (baseline model EB6), (b) CS walls crack patterns for configurations C1/C2

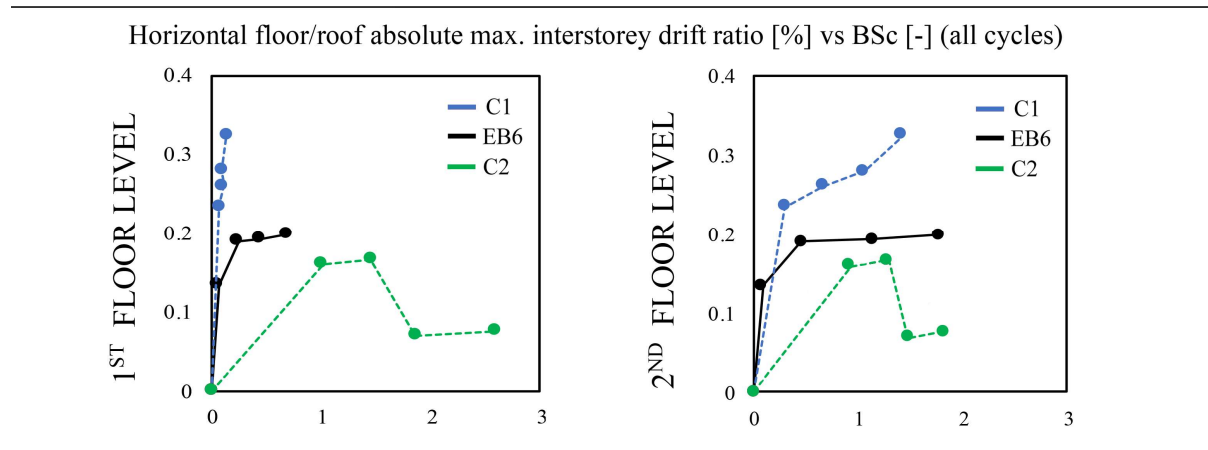


Fig. 6 Predicted 1st and 2nd horizontal floor/roof absolute max. interstorey drift ratios vs. BSc for each cycle and comparison with experimental counterparts (baseline model EB6)



## 5. Conclusions

In this paper, the influence of the extent of ground floor openings on the response of typical Dutch unreinforced masonry (URM) terraced houses was investigated using a micro-modeling strategy, implemented in an Applied Element Method (AEM)-based computational platform, whose unique features enabled a comprehensive parametric study to be carried out in a reasonable timeframe and to represent explicitly damage initiation and propagation until up to complete collapse.

Firstly, a preliminary assessment of the effectiveness of the adopted modeling strategy is proposed, taking as a reference the experimental shake-table results of a full-scale cavity-wall building specimen (i.e. EUC-BUILD6). Given the adequate agreement found among actual and modeled dynamic behavior, the response of a number of additional geometrical configurations, characterized by different ground floor opening percentages and subjected to the same incremental uniaxial loading protocol employed for EUC-BUILD6, was then investigated.

The analysis outcomes, summarized herein but further detailed in [21], confirm that the extent of ground floor openings may affect significantly the dynamic performance of the considered URM building typology, with the overall strength capacity of the latter decreasing with increasing openings percentage, which also causes deformations and failure mechanisms to concentrate on the ground floor. Future enhancements may include comparisons in terms of produced post-collapse debris field, as well as the development of ensuing fragility functions to study potential dissimilarities in the seismic vulnerability of URM terraced houses with different opening percentages [22].

## 6. Acknowledgments

The work described in this paper was carried out within the framework of the research program on hazard and risk of induced seismicity in the Groningen region, sponsored by the Nederlandse Aardolie Maatschappij BV (NAM). The authors also acknowledge all those at both the European Centre for Training and Research in Earthquake Engineering (Eucentre, Pavia, Italy) that were involved in the testing campaign referred to in this paper, and in particular Francesco Graziotti, Gabriele Guerrini, Marco Miglietta, Luca Grottoli and Nicolò Damiani for their precious assistance in accessing the test data. Finally, the collaboration of the technical support staff from Applied Science International LLC (ASI), on the use of the employed AEM software - Extreme Loading for Structures, is also acknowledged.

## 7. References

- [1] Graziotti F, Penna A, Magenes G (2019): A comprehensive in situ and laboratory testing programme supporting seismic risk analysis of URM buildings subjected to induced earthquakes. *Bulletin of Earthquake Engineering*, 17(8): 4575–4599. DOI: 10.1007/s10518-018-0478-6.
- [2] Graziotti F, Tomassetti U, Kallioras S, Penna A, Magenes G (2017): Shaking table test on a full scale URM cavity wall building. *Bulletin of Earthquake Engineering*, 15(12): 5329–5364. DOI: 10.1007/s10518-017-0185-8.
- [3] Miglietta M, Damiani N, Grottoli L, Guerrini G, Graziotti F (2019): Shake-table investigation of a timber retrofit solution for unreinforced masonry cavity-wall buildings. *In Proceedings of the XVIII ANIDIS Conference*, Ascoli Piceno, Italy: Pisa University Press. DOI: 10.1400/271082.
- [4] Malomo D, Pinho R, Penna A (2020): Simulating the shake-table response of URM cavity-wall structures tested to collapse or near-collapse conditions. *Earthquake Spectra* - in press. DOI: 10.1177/8755293019891715.
- [5] Meguro K, Tagel-Din H (2000): Applied element method for structural analysis: Theory and application for linear materials. *Structural Engineering/Earthquake Engineering*, 17(1).
- [6] Meguro K, Tagel-Din H (2001): Applied Element Simulation of RC Structures under Cyclic Loading. *Journal of Structural Engineering*, 127(11): 1295–1305. DOI: 10.1061/(ASCE)0733-9445(2001)127:11(1295).
- [7] Meguro K, Tagel-Din H (2002): Applied Element Method Used for Large Displacement Structural Analysis.



*Journal of Natural Disaster Science*, 24(1): 25–34.

- [8] Malomo D, Pinho R, Penna A (2018): Using the applied element method for modelling calcium silicate brick masonry subjected to in-plane cyclic loading. *Earthquake Engineering & Structural Dynamics*, 47(7): 1610–1630. DOI: 10.1002/eqe.3032.
- [9] Garofano A, Lestuzzi P (2016): Seismic Assessment of a Historical Masonry Building in Switzerland: The “Ancien Hôpital De Sion” *International Journal of Architectural Heritage*, 10(8): 975–992. DOI: 10.1080/15583058.2016.1160303.
- [10] Karbassi A, Nollet MJ (2013): Performance-based seismic vulnerability evaluation of masonry buildings using applied element method in a nonlinear dynamic-based analytical procedure. *Earthquake Spectra*, 29(2): 399–426.
- [11] Lourenço PB, Rots JG (1997): Multisurface Interface Model for Analysis of Masonry Structures. *Journal of Engineering Mechanics*, 123(7): 660–668. DOI: 10.1061/(ASCE)0733-9399(1997)123:7(660).
- [12] Jäger W, Irmschler H, Schubert P (2004). *Mauerwerk-Kalender*. Ernst & Sohn Verlag für Architektur und technische Wissenschaften.
- [13] Kaushik HB, Rai DC, Jain SK (2007): Stress-strain characteristics of clay brick masonry under uniaxial compression. *Journal of Materials in Civil Engineering*, 19(9): 728–739.
- [14] Brooks JJ, Baker A (1998): Modulus of Elasticity of Masonry. *Masonry International*, 12(2): 58–63.
- [15] Matysek P, Janowski Z (1996) Analysis of factors affecting the modulus of elasticity of the walls. *In Proceedings of the Conference of the Committee of Civil Engineering PZITB*, Lublin, Poland.
- [16] Ciesielski R (1999): The dynamic module of elasticity of brick walls. *In Proceedings of the Conference of the Committee of Civil Engineering PZITB*, Lublin, Poland.
- [17] U.B.C. - Uniform Building Code (1991), Whittier, CA, United States.
- [18] Messali F, Esposito R, Maragna M (2016): Pull-out strength of wall ties. *Technical Report*, TU Delft, The Netherlands. Available from URL: <http://www.nam.nl/feiten-en-cijfers/onderzoeksrapporten.html>.
- [19] Ravenshorst G, de Vries P (2018): Cyclic testing of trial timber diaphragm. *Technical Report*, TU Delft, The Netherlands. Available from URL: <http://www.nam.nl/feiten-en-cijfers/onderzoeksrapporten.html>.
- [20] Arup. (2019): *Technical Report 229746\_031.0\_REP2014 - Exposure Database v6*. Available from URL: <http://www.nam.nl/feiten-en-cijfers/onderzoeksrapporten.html>.
- [21] Mosayk (2019): Impact of ground floor openings percentage on the response of a terraced house unit model. *Modelling Report n. D11 - Revision 22 January 2019*. Available from URL: <http://www.nam.nl/feiten-en-cijfers/onderzoeksrapporten.html>.
- [22] Malomo D, Morandini C, Penna A, Crowley H, Pinho R (2020): Impact of ground floor openings percentage on the dynamic response of URM cavity-wall structures. *Bulletin of Earthquake Engineering* - submitted for publication.